Axion emission rates in stars and constraints on its mass

Anthony Pantziris and Kyungsik Kang
Department of Physics, Brown University, Providence, Rhode Island 02912
(Received 24 December 1985)

We have calculated in detail the emission rates of the invisible axion of Dine, Fischler, and Srednicki in several representative types of stars and derived upper bounds for its mass. We give, in particular, complete reaction amplitudes and energy rates for axion emission. Our results for the axion mass limits are in qualitative agreement with previous estimates for most of the cases except for the neutron stars which give a stronger bound on the axion mass.

I. INTRODUCTION

Although the invisible axion was proposed to be a natural solution to the strong *CP* problem,[1] its mass in the Dine, Fischler, and Srednicki (DFS) model[2] is left undetermined. Since the coupling of this axion to matter is presumably very weak, laboratory experiments are unable to detect it and one can derive only bounds on its mass from astrophysical considerations. In our calculations we have extended the work of Fukugita, Watamura, and Yoshimura,[3] which concentrated for the most part in the nondegenerate and nonrelativistic electron gas region, and the work of Iwamoto,[4] which examined axion emission in neutron stars, to most of the significant regions, typical for hydrogen-burning stars, helium-burning stars, carbon- and oxygen-burning stars, supernovae, and neutron stars. The plasmon effects are always included in the relevant reactions, and the axion mass is not neglected at low temperatures.

We examine in detail the annihilation process $e^+ + e^- \to \gamma + a$, the Primakoff reaction $(Z,e) + \gamma \to (Z,e) + a$, the Compton process $e + \gamma \to e + a$, and the plasma decay $\gamma_{\rm pl} \to \gamma + a$, in all of the above regions, and axion bremsstrahlung of the Compton and Primakoff type $e + (Z,A) \to e + (Z,A) + a$ and from neutron-neutron collisions $n + n \to n + n + a$, in degenerate regions (Fig. 1).

The axion couples to matter through a pseudoscalar interaction and the interaction Lagrangian is given, in the notation of Refs. 2 and 3, by

$$L_a = \frac{2i}{v_\phi}\left[\frac{1}{x^2+1} M_u \bar{u}\gamma_5 u a + \frac{x^2}{x^2+1}(M_d \bar{d}\gamma_5 d a + M_e \bar{e}\gamma_5 e a)\right] \quad (1.1)$$

and similarly for heavier generations. The parameter x is arbitrary in the model and we choose the simplifying value $x=1$. The axion couples to photons through a fermion loop and the effective vertex is

$$T(a \to 2\gamma) = \frac{\alpha}{8\pi}\mathrm{Tr}(Q_5^a Q^2) F_{\mu\nu}\tilde{F}^{\mu\nu}, \quad (1.2)$$

where Q_5^a is the $U(1)_{PQ}$ charge[1] and Q is the electric charge generator. Using current-algebra methods, the trace is calculated to be[5]

$$\mathrm{Tr}(Q_5^a Q^2) = \frac{2}{v_\phi}\frac{Nz}{1+z},$$

where N is the number of generations, which is taken to be three in our calculations, and $z = \langle M_u \bar{u}u \rangle / \langle M_d \bar{d}d \rangle = 0.56$.

II. EMISSION RATES

The axion emission rates are calculated for each reaction by integrating the spin-summed squared matrix element, weighted by the axion emitted energy, over the total final and initial phase space available, taking care of the

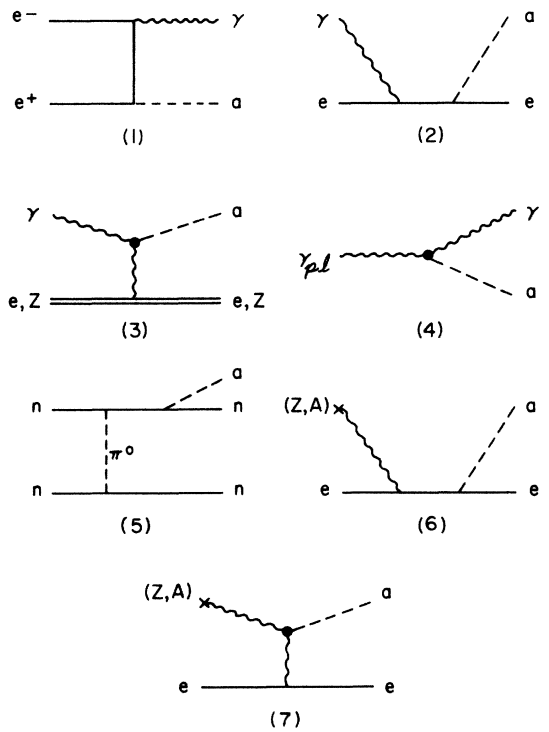

FIG. 1. Axion emission processes in stars: (1) e^+e^- annihilation process; (2) Compton process; (3) Primakoff process; (4) plasma decay; (5) neutron-neutron axion bremsstrahlung; (6) Compton-type axion bremsstrahlung; (7) Primakoff-type axion bremsstrahlung.

screening due to fermion degeneracy in the final states. Axion reabsorption is negligible since the mean free path of the axion is much larger than the sizes of stars for the range of the axion mass that we consider.[3]

The number densities of fermions and photons are given by

$$dn_{\pm}=\frac{2}{(2\pi)^3}d^3p\, n_{\pm}(p)\,,$$
$$dn_{\gamma}=\frac{2}{(2\pi)^3}d^3p(e^{E/T}-1)^{-1}\,, \tag{2.1}$$

where $n_{\pm}(p)$ is the Fermi function $(e^{(E\pm\mu)/T}+1)^{-1}$. Throughout this paper we use the natural units in which $c=\hbar=k_B=1$. From the requirement of charge neutrality we get

$$n_{-}-n_{+}=N_A\frac{\rho}{\mu_e}\,, \tag{2.2}$$

where

$$\mu_e^{-1}=\sum_i\frac{X_iZ_i}{A_i}\,,$$

N_A is Avogadro's number, X_i is the chemical composition parameter, and ρ the density in units of $\mathrm{g\,cm^{-3}}$. At high densities and relatively low temperatures the photon acquires an effective mass: $E_\gamma^2\simeq\omega^2+\mathbf{k}^2$, due to constant interaction with the electron gas, which is given by[6]

$$\left[\frac{\omega}{M_e}\right]^2=\frac{4\alpha}{3\pi}\lambda^2\int_{1/\lambda}^{\infty}dx\left[x^2-\frac{1}{\lambda^2}\right]^{1/2}\times\left[2+\frac{1}{\lambda^2x^2}\right](e^{x-\nu}+1)^{-1}\,, \tag{2.3}$$

for transverse plasmons. Here $\alpha=e^2/4\pi$, $\lambda=T/M_e$, and $\nu=\mu/T$. Longitudinal plasmons become important when both electron and positron gases are relativistic. The dispersion relation for longitudinal plasmons is then given by

$$E^2\simeq\omega^2+\tfrac{3}{5}\mathbf{k}^2\,. \tag{2.4}$$

A. e^+e^- annihilation process

The lowest-order Feynman diagram is depicted in Fig. 1(1) and the energy loss per unit mass for the reaction $e^+(p_2)+e^-(p_1)\rightarrow\gamma(k)+a(k_a)$ is given by

$$\epsilon_a=\frac{1}{\rho}\int\frac{dn_+}{2E_2}\frac{dn_-}{2E_1}\int\frac{d^3k_a}{2k_a^0}\frac{d^3k}{2k^0}(2\pi)^{-2}\times\delta^4(p_1+p_2-k-k_a)k_a^0\,|M'|^2\,. \tag{2.5}$$

The amplitude is conveniently calculated in the rest frame of the electron:

$$|M'|^2=(ge)^2\frac{(M_e+E_2)^2}{E_a(E_2+M_e-E_a)}\times\left[1+\frac{m_a^2(E_2-E_a)}{2M_eE_a(M_e+E_2-E_a)}\right], \tag{2.6}$$

where $g=M_e/v_\phi=1.41\times10^{-11}\ m_a/\mathrm{eV}$. It turns out that the term multiplied by m_a^2 is important only at high temperatures $T>M_e$, but then $(m_a/T)^2\ll1$, so we can neglect it in all regions. After integration of the final states we obtain

$$\epsilon_a=\frac{g^2\alpha}{32\pi^4\rho}\int\frac{dp_1p_1^2}{e^{(E_1-\mu)/T}+1}\frac{dp_2p_2^2}{e^{(E_2+\mu)/T}+1}d\cos\theta_{12}\times\left[\frac{1}{E_1}+\frac{1}{E_2}\right]U^{-1}(u+1+vu)\times\ln\left[\frac{1+U}{1-U}\right], \tag{2.7}$$

where $u=p_1\cdot p_2/M_e^2$, $v=\mathbf{p}_1\cdot\mathbf{p}_2/E_1E_2$, and $U=[(u-1)/(u+1)]^{1/2}$. To bring it in this form we made a Lorentz boost to an arbitrary frame. Now we calculate the emission rate given by Eq. (2.7) in various physical regions.

(i) Nonrelativistic and mildly degenerate electron gas, $\mu\simeq M_e$. This is the case for $T<10^7$ K and $\rho<10^4\ \mathrm{g\,cm^{-3}}$ or $T\simeq10^9$ K and $\rho\simeq10^6\ \mathrm{g\,cm^{-3}}$, see Ref. 7. Then Eq. (2.7) gives

$$\epsilon_a=g^2\alpha e^{-2M_e/T}\frac{M_e^2T^3}{4\rho\pi^3}\left[1-\frac{1}{\sqrt{2}}\right]\zeta\left[\frac{3}{2}\right]\times\left[1+\frac{T}{4M_e}\left[1+\frac{\left[1-\frac{1}{2\sqrt{2}}\right]\zeta(\frac{5}{2})}{\left[1-\frac{1}{\sqrt{2}}\right]\zeta(\frac{3}{2})}\right]\right]. \tag{2.8}$$

Here ζ is the Riemann zeta function.

(ii) Nonrelativistic and nondegenerate electron gas, $T<M_e$ and $\mu\ll M_e$. This is true for $\rho<10^5\ \mathrm{g\,cm^{-3}}$ and $10^8<T<10^9$ K with higher densities requiring higher temperatures.[7] The emission rate becomes

$$\epsilon_a=g^2\alpha\frac{M_e^2T^3}{4\rho\pi^3}e^{-2M_e/T}\left[1+\frac{T}{2M_e}\right]. \tag{2.9}$$

This agrees with the result of Ref. 3 in the limit $T/M_e\rightarrow0$.

(iii) Nonrelativistic but degenerate electron gas, $M_e/T\ll\mu/T\ll2M_e/T$. This is the case for $T<10^8$ K and $10^4<\rho<10^6\ \mathrm{g\,cm^{-3}}$. We get

$$\epsilon_a=g^2\alpha\frac{M_e^2T^3}{\rho\pi4}e^{-(M_e+\mu)/T}\times\int_0^{\infty}\frac{dx\sqrt{x}}{e^{x-\nu+1/\lambda}+1}\int_0^{\infty}\frac{dy\sqrt{y}}{e^y}\left[1+\frac{x+y}{6}\frac{T}{M_e}\right]. \tag{2.10}$$

(iv) Electron gas is very relativistic and degenerate but positron gas is nonrelativistic . This is the region for which $10^{10}>T>10^8$ K, and $10^{15}>\rho>10^{12}\ \mathrm{g\,cm^{-3}}$, such as the interior of neutron stars. Equation (2.7) reduces to

$$\epsilon_a = g^2\alpha e^{-(M_e+\mu)/T}\left[\frac{M_e{}^{1/2}T^{9/2}\sqrt{2\pi}}{4\rho\pi^4}\right] \times \int_0^\infty \frac{dx\,x^2}{e^{x-\nu}+1}\left[1+\frac{2M_e}{xT}\right]\left[\ln\frac{2xT}{M_e}-\frac{M_e}{2xT}\right]. \tag{2.11}$$

(v) Electron gas and positron gas are relativistic, $\mu \gg T > M_e$. This is true for $T > 10^{10}$ K and $10^{10} > \rho > 10^8$ g cm^{-3}, the conditions of a supernova explosion. We obtain

$$\epsilon_a = g^2\alpha\frac{T^7 e^{-\mu/T}}{12\rho\pi^4 M_e{}^2} \times \int_{1/\lambda}^\infty \frac{dx\,x^2(x^2-\lambda^{-2})^{1/2}}{e^{x-\nu}+1} \times \int_{1/\lambda}^\infty \frac{dy\,y(y^2-\lambda^{-2})^{1/2}}{e^y} \times \left[\ln xy + 2\ln\frac{2T}{M_e}-\frac{5}{6}\right]. \tag{2.12}$$

Note that for the cases of (iii), (iv), and (v) numerical integration is needed for the emission rates.

B. Compton process

The energy-loss rate per unit mass for the reaction $e(p_1)+\gamma(k)\rightarrow e(p_2)+a(k_a)$, Fig. 1(2), is given by

$$\epsilon_c = \frac{1}{\rho}\int\frac{dn_-}{2E_1}\frac{dn_\gamma}{2E_\gamma}\int\frac{d^3k_a}{2k_a^0}\frac{d^3p_2}{2E_2}(2\pi)^{-2}[1-n(E_2)] \times \delta^4(p_1+k-p_2-k_a)E_a\,|M'|^2. \tag{2.13}$$

The factor $1-n(E_2)$ comes from screening due to Fermi statistics. In the rest frame of the initial electron, keeping the terms up to the first order in $m_a{}^2$, the spin summed squared matrix element is

$$|M'|^2=(ge)^2\left\{\frac{E_a}{E_\gamma+\frac{\omega^2}{2M_e}}+\frac{E_\gamma+\frac{\omega^2}{2M_e}}{E_a}-2+\frac{m_a{}^2}{2M_e}\left[\frac{E_\gamma}{E_a{}^2}-\frac{E_\gamma}{\left[E_\gamma+\frac{\omega^2}{2M_e}\right]^2}+\frac{\omega^2}{M_eE_a{}^2}-\frac{\omega^2}{M_eE_a\left[E_\gamma+\frac{\omega^2}{2M_e}\right]}\right] - \left[\frac{\omega^2/2M_e{}^2}{E_a\left[E_\gamma+\frac{\omega^2}{2M_e}\right]}+\frac{m_a{}^2}{2M_e{}^2E_a{}^2}\left[\frac{E_\gamma+\omega^2/M_e}{E_\gamma+\omega^2/2M_e}\right]\right] \times\left[\frac{(E_\gamma{}^2-\omega^2)(E_a{}^2-m_a{}^2)-[M_e(E_a-E_\gamma)+E_aE_\gamma-(m_a{}^2+\omega^2)/2]^2}{E_\gamma{}^2-\omega^2}\right]\right\}, \tag{2.14}$$

where ω is the plasmon effective mass. This reduces to the approximate result of Ref. 3 in the limit $m_a{}^2=\omega^2=0$. Only transverse plasmons are significant in the examined regions. In order to give analytic expressions of the energy-loss rate we examine three regions.

(i) $T < 10^7$ K and $\rho < 10^4$ g cm^{-3}. Then $\omega, m_a < T \ll M_e$, so we can expand in ω^2 and $m_a{}^2$ and keep the terms up to first order. The result is

$$\epsilon_c = \frac{g^2\alpha}{3\pi^2}\frac{N_A}{\mu_e}\frac{T^6}{M_e{}^4}\int_{\omega/T}^\infty \frac{dx\left[x^2-\frac{\omega^2}{T^2}\right]^{1/2}}{e^x-1}\left[x^4+\frac{14}{3}x^4\frac{\langle p_1{}^2\rangle}{M_e{}^2}-\frac{6x^5T}{M_e}-\left[m_a{}^2+\frac{\omega^2}{2}\right]\frac{x^2}{T^2}\right], \tag{2.15}$$

where $\langle p_1{}^2\rangle = \int dn_-\,p_1{}^2/\int dn_-$. This holds for nonrelativistic and mildly degenerate electron gas.

(ii) $10^6 < T < 5\times10^8$ K and $\rho < 10^7$ g cm^{-3}. In this region we can neglect safely the axion mass and we can still consider the electrons as approximately nonrelativistic or mildly relativistic with higher densities requiring higher temperatures. The energy rate is

$$\epsilon_c = \frac{g^2\alpha}{3\mu_e\pi^2}[1-n(M_e)]N_A\frac{T^6}{M_e{}^4}\int_\Omega^\infty \frac{dx\,(x^2-\Omega^2)^{1/2}}{e^x-1}\left[x^4-\frac{x^2\Omega^2}{2}-\frac{T}{M_e}\left[6x^5-5x^3\Omega^2+x\frac{\Omega^4}{2}\right] + \frac{\langle p_1{}^2\rangle}{M_e{}^2}\left[\frac{14x^4}{3}-\frac{10x^2\Omega^2}{3}+\frac{\Omega^4}{6}\right]\right], \tag{2.16}$$

where $\Omega=\omega/T$. Plasmon effects can be important for this region.

(iii) $10^8<T<10^{10}$ K and $10^{11}<\rho<10^{15}$ g cm^{-3}. In this region the electron gas is very relativistic and degenerate. Also $\omega\gg T$ so the transverse plasmon effects are very important. Longitudinal plasmons are also present but the correction is small. The energy-loss rate is

$$\epsilon_c=\frac{g^2\alpha}{3\mu_e\pi^2}[1-n(P_F)]N_A T^2 \times\int_\Omega^\infty \frac{dx\,(x^2-\Omega^2)^{1/2}}{e^x-1} \times\frac{B^4\left[B+\frac{P_F}{M_e}\right]^2\left[\frac{B}{2}+\frac{P_F}{M_e}\right]^2}{\left[1+2B\frac{P_F}{M_e}+B^2\right]^3}, \quad (2.17)$$

where P_F is the Fermi energy of the electron gas, so that $n(P_F)=\frac{1}{2}$ and $B=\omega/M_e$. For large densities the energy rate decreases exponentially like $e^{-\omega/T}$.

C. Primakoff process

The energy-loss rate per unit mass for the reaction $Z,e(p_1)+\gamma(k)\rightarrow Z,e(p_2)+a(k_a)$, see Fig. 1(3), is the sum of the contributions from atomic electrons and nuclei, $\epsilon_p=\epsilon_p(e)+\epsilon_p(Z)$. The emission rate for this process is

$$\epsilon_p=\frac{1}{\rho}\sum_{e,Z}\int\frac{dn_1}{2E_1}\frac{dn_\gamma}{2E_\gamma}\int\frac{d^3p_2}{2E_2}\frac{d^3k_a}{2E_a}(2\pi)^{-2} \times\delta^4(p_1-p_2+k-k_a)\,|M'|^2 \times E_a[1-n(p_2)]\,. \quad (2.18)$$

The effective $a\gamma\gamma$ vertex is

$$T_{\mu\nu}{}^5=\frac{2\alpha c}{\pi v_\phi}\epsilon_{\mu\nu\rho\sigma}k^\rho k^\sigma\,,$$

$$\frac{2c}{v_\phi}=\mathrm{Tr}(Q_5Q^2)\,.$$

The spin-summed squared matrix element in the rest frame of the initial electron (or nucleus) is

$$|M'|^2=\frac{16\alpha^3c^2}{\pi v_\phi{}^2}\left[-\frac{M^2}{2}+\frac{M}{2}\frac{E_\gamma{}^2+E_a{}^2}{E_\gamma-E_a}-\frac{M}{2}\frac{\omega^2+m_a{}^2}{E_\gamma-E_a} -\frac{(\omega^2-m_a{}^2)^2}{8(E_\gamma-E_a)^2}+\frac{\omega^2E_\gamma}{2(E_\gamma-E_a)} -\frac{m_a{}^2E_a}{2(E_\gamma-E_a)}\right] \quad (2.19)$$

which reproduces the result of Ref. 3 if the recoil effect is neglected and $\omega=0$. Here M is the mass of the participating electron or nucleus. As before we consider three regions of interest and derive expressions for the emission rate.

(i) $T<10^7$ K and $\rho<10^4$ g cm^{-3}. Then $m,\omega<T\ll M$ and we keep the terms up to first order in $m_a{}^2$ and ω^2. The result is

$$\epsilon_p=\frac{2\alpha^3c^2}{\pi^4v_\phi{}^2}\frac{N_A}{\mu_e'}T^4\int_\Omega^\infty\frac{dx\,(x^2-\Omega^2)^{1/2}}{e^x-1}\left[x^2\left[\ln\frac{2xT}{(\omega^2-m_a{}^2)^{1/2}}-\frac{1}{2}\right]-\frac{\Omega^2}{4}-\frac{m_a{}^2}{2T^2}\ln\frac{2Tx}{(\omega^2-m_a{}^2)^{1/2}}\right], \quad (2.20)$$

where

$$\frac{1}{\mu_e'}=\sum_i X_iZ_i(Z_i+1)/A_i\,.$$

(ii) $10^6<T<5\times10^8$ K and $\rho<10^8$ g cm^{-3}. In this region we can neglect the axion mass and treat the electrons as approximately nonrelativistic. The nuclei are nonrelativistic. We get

$$\epsilon_p=\frac{2\alpha^3c^2T^4}{\pi^4v_\phi{}^2}N_A\int_\Omega^\infty\frac{dx\,x^2(x^2-\Omega^2)^{1/2}}{e^x-1} \times\left[\frac{1}{\mu_e'}\left[-\frac{1}{2}+\frac{x^2-\Omega^2/2}{x(x^2-\Omega^2)^{1/2}}\ln\left[\frac{x+(x^2-\Omega^2)^{1/2}}{\Omega}\right]\right] +[1-n(M_e)]\frac{1}{\mu_e}\left\{-\frac{3}{4}x\left[1-\frac{\Omega^2}{x^2}\right]\frac{T}{M_e} +\frac{2}{3}\frac{\langle p_1{}^2\rangle}{M_e{}^2}\left[\frac{1}{(1-\Omega^2/x^2)^{1/2}}\ln\left[\frac{x+(x^2-\Omega^2)^{1/2}}{\Omega}\right]+\frac{3}{4}\left[1-\frac{\Omega^2}{x^2}\right]\right]\right\}\right]. \quad (2.21)$$

The second term is due only to the electron contribution.

(iii) $10^8 < T < 10^{10}$ K and $10^{11} < \rho < 10^{15}$ g cm^{-3}. Here $\omega \gg T$ and the electrons are very relativistic and degenerate. The nuclei are considered to be nonrelativistic and their contribution is given by the first term of Eq. (2.21), with the substitution $1/\mu_e' \to 1/\mu_e' - 1/\mu_e$. The electron contribution is ($\gamma = P_F/M_e$)

$$\epsilon_p(e) = \frac{\alpha^3 c^2}{\pi^4 v_\phi^2} \frac{M_e^2 N_A}{\mu_e} T^2 \times \int_\Omega^\infty \frac{dx\,(x^2-\Omega^2)^{1/2}}{e^x - 1} \times \frac{B^4(B\gamma+1)^2(B\gamma+\frac{3}{2})(\gamma+B/2)^2}{(1+2B\gamma+B^2)^3} . \tag{2.22}$$

For high densities the energy loss becomes small like $e^{-\omega/T}$. Correction due to the presence of longitudinal plasmons is negligible.

D. Plasma decay process

Transverse plasmons can decay via $\gamma_{\rm pl}(k_{\rm pl}) \to \gamma(k) + a(k_a)$ and the energy-loss rate per unit mass of the star is [see Fig. 1(4)]

$$\epsilon_{\rm pl} = \frac{1}{\rho} \int \frac{dn_{\rm pl}}{2E_{\rm pl}} \int \frac{d^3k_a}{2E_a} \frac{d^3k}{2k} (2\pi)^{-2} \times \delta^4(k_{\rm pl} - k - k_a)\,|M'|^2 E_a . \tag{2.23}$$

The effective $\gamma_{\rm pl}\gamma a$ vertex is the same as that in the Primakoff process [Fig. 1(3)].

For $\omega < 2M_i$, where M_i are lepton or quark masses, the squared amplitude is

$$|M'|^2 = \frac{c^2\omega^2}{4v_\phi^2\pi^4} \left[1 - \frac{m_a^2}{\omega^2}\right]^{-2} k^2 \sin^2\theta , \tag{2.24}$$

where θ is the angle between $\mathbf{k}$ and $\mathbf{k}_{\rm pl}$. The energy-loss rate due to transverse plasmon decay is

$$\epsilon_{\rm pl}(t) = \frac{\alpha^2\omega^4 c^2 T^3}{48\rho\pi^5 v_\phi^2} \left[1 - \frac{m_a^2}{\omega^2}\right] \times \int_\Omega^\infty \frac{dx\,x\,(x^2-\Omega^2)^{1/2}}{e^x - 1} . \tag{2.25}$$

Longitudinal plasmons become significant when the electron and positron gases become relativistic.[6] The energy-loss rate is

$$\epsilon_{\rm pl}(l) = \frac{\alpha^2 c^2 T^7}{48\rho\pi^5 v_\phi^2} \left[\frac{5}{3}\right]^{3/2} \int_\Omega^\infty \frac{dx\,x^5 (x^2-\Omega^2)^{1/2}}{e^x - 1} \tag{2.26}$$

with $\omega \gg T$, so that it decreases like $e^{-\omega/T}$. In our physical regions we always have $\omega \ll 2M_i$ for most of the fermions.

E. Neutron-neutron axion bremsstrahlung

The Feynman diagram for this process is shown in Fig. 1(5) and the one-pion-exchange model is used for the neutron-neutron scattering. The axion-neutron effective Lagrangian is $L_{nna} = ig n \gamma_5 n a$ where $g = C_a M_n / v_\phi$, with $C_a = 1.25$, the axial-vector renormalization constant. The energy-loss rate per unit mass for the reaction $n(p_1) + n(p_2) \to n(p_3) + n(p_4) + a(p_5)$ is

$$\epsilon_{nn} = \frac{1}{2\rho} \left[\prod_{i=1}^5 \int \frac{d^3p_i}{2E_i}\right] n(p_1) n(p_2) [1 - n(p_3)] \times [1 - n(p_4)] (2\pi)^{-11} \times \delta^4(p_1 + p_2 - p_3 - p_4 - p_5)\,|M'|^2 E_5 . \tag{2.27}$$

In the nonrelativistic limit the spin summed squared matrix element is

$$|M'|^2 = 512 g^2 \left[\frac{f}{\mu_\pi}\right]^4 M_n^{*4} \left[\frac{|\mathbf{p}_1 - \mathbf{p}_3|^2}{(|\mathbf{p}_1 - \mathbf{p}_3|^2 + \mu_\pi^2)^2} + \frac{|\mathbf{p}_1 - \mathbf{p}_4|^2}{(|\mathbf{p}_1 - \mathbf{p}_4|^2 + \mu_\pi^2)^2}\right] , \tag{2.28}$$

where μ_π is the pion mass, M_n^* the neutron effective mass $f \simeq 1.00$, and the

$$O(|\mathbf{p}_1 - \mathbf{p}_3|^4 / M_n^{*2} (|\mathbf{p}_1 - \mathbf{p}_3|^2 + \mu_\pi^2)^2)$$

terms are neglected. Assuming neutron degeneracy we can use the technique by Friman and Maxwell[8] to calculate the energy-loss rate:

$$\epsilon_{nn} = \frac{31 g^2}{1890\pi\rho} \left[\frac{f}{\mu_\pi}\right]^4 \left[\frac{M_n^*}{\mu_\pi}\right]^2 M_n^{*2} P_F T^6 \times \left[-\frac{2x^2}{1+x^2} + 2x \arctan\frac{1}{x}\right] , \tag{2.29}$$

where $x = \mu_\pi / 2P_F$ and P_F is the neutron Fermi momentum. The axion mass is at these energies neglected compared to neutron or pion mass. We get here a different result from the work of Iwamoto which results to a stronger bound of the axion mass.[9]

F. Compton-type axion bremsstrahlung

This process, see Fig. 1(6), occurs with the interaction of the degenerate electrons with a Coulomb field of the nuclei which are assumed to be fixed. This field is weakly screened:

$$A^{\mu}=\frac{Ze}{4\pi}\frac{e^{-rq_{sc}}}{r}g_{\mu 0}\ , \tag{2.30}$$

where $q_{sc}=\sqrt{4\alpha/\pi}P_F(e)$. The energy-loss rate per unit mass for the reaction $e(p_1)+(Z,A)\rightarrow e(p_2)+(Z,A)+a(k_a)$ is

$$\epsilon_{cb}=\frac{1}{AM_p}\int\frac{dn_1}{2E_1}d^3q\int\frac{d^3p_2}{2E_2}\frac{d^3k_a}{2E_a}[1-n(p_2)](2\pi)^{-5}\times\delta^4(p_1+q-p_2-k_a)\,|M'|^2E_a\ , \tag{2.31}$$

where M_p the proton mass and $\mathbf{q}$ the momentum of the Coulomb field. The spin-summed squared matrix element, assuming strong electron degeneracy is given by

$$|M'|^2=\frac{2Z^2e^4g^2\beta^2}{(q_{sc}^2+\mathbf{q}^2)^2}\left[\frac{\cos\theta_{2a}\cos\theta_{1a}+1-\cos\theta_{12}-\frac{1}{2}(\cos^2\theta_{1a}+\cos^2\theta_{2a})}{(1-\beta\cos\theta_{1a})(1-\beta\cos\theta_{2a})}\right], \tag{2.32}$$

where $\beta=P/E$ and the subscript a denotes the axion. Analytical and simple expressions for the emission rate can be derived for various limiting cases. For example, very relativistic electrons give the emission rate

$$\epsilon_{cb}=\frac{\pi^2\alpha}{120}\frac{Z^2g^2}{AM_p}\frac{T^4}{P_F^2}(2\ln 2\gamma-1) \tag{2.33}$$

with $\gamma=(1-\beta^2)^{-1/2}$, a result reached by Iwamoto[4] recently. For nonrelativistic electrons $[\beta=\beta(P_F)]$, we obtain

$$\epsilon_{cb}=\frac{\pi^2\alpha}{90}\frac{Z^2g^2}{AM_p}\frac{T^4}{P_F^2}\beta^4\ . \tag{2.34}$$

G. Primakoff-type axion bremsstrahlung

In this process, Fig. 1(7), the axion is emitted by the screened, static Coulomb field, which is interacting with the electron gas. The energy-loss rate per unit mass for $e(1)+(Z,A)\rightarrow e(2)+(Z,A)+a$, Primakoff type, is given by

$$\epsilon_{pb}=\frac{1}{AM_p}\int\frac{dn_1}{2E_1}d^3k\int\frac{d^3p_2}{2E_2}\frac{d^3k_a}{2E_a}(2\pi)^{-5}\times\delta^4(p_1+k-p_2-k_a)\,|M'|^2E_a\times[1-n(p_2)]\ . \tag{2.35}$$

For very degenerate electrons the spin-summed squared amplitude is

$$|M'|^2=\frac{2(8Z\alpha^2c)^2}{(\mathbf{k}^2+q_{sc}^2)^2}\frac{k_a^2P_F^4}{v_\phi^2q^4}\times[4(1-\cos\theta_{12})(\cos\theta_{2a}\cos\theta_{1a}-\cos\theta_{12})+(1+\cos\theta_{12})(\cos\theta_{2a}-\cos\theta_{1a})^2] \tag{2.36}$$

where $q=p_1-p_2$ and a denotes the axion. Then the energy-loss rate per unit mass is computed to be, using the Sommerfeld expansion,

$$\epsilon_{pb}=\frac{2\pi^2}{189}\frac{Z^2\alpha^3}{AM_p}\frac{c^2\beta^2}{v_\phi^2}\frac{T^6}{P_F^2}\left[1+\frac{\alpha}{\pi}\ln\frac{\alpha}{\pi}\right], \tag{2.37}$$

where $\beta=\beta(P_F)$. This rate is smaller than the Compton-type rate, due to the factor α^3.

III. AXION EMISSION IN STARS

In this section we examine, with the emission rates obtained in the preceding section, stars at various stages of evolution. We can get an upper bound on the axion mass by requiring that the emission rates due to axions either are smaller than the nuclear energy generation in the interior of the stars or, if such energy generation is not known accurately and safely, as in the cases of white dwarfs and neutron stars, the emission rates do not violate the standard neutrino emission scenario which is in agreement with observations.[10,11]

A. Hydrogen-burning stars

Among hydrogen-burning stars the Sun is selected since its physical parameters are best known. The interior temperature is around 10^7 K and the density about 10^2 g cm^{-3} so the electron gas is mildly degenerate and nonrelativistic. Plasma effects are small since $\omega/T\sim 0.2$, see Fig. 2, for the relevant region, becoming stronger at lower temperatures. The Primakoff process and the Compton process contribute to the energy loss, while the annihilation and the plasma decay processes are negligible, see Fig. 3. We require

$$\int_0^{M_\odot}dM(r)\sum_i\epsilon_i(\rho,T,C)<\epsilon_N=3.86\times 10^{33}\ \text{erg sec}^{-1}\ , \tag{3.1}$$

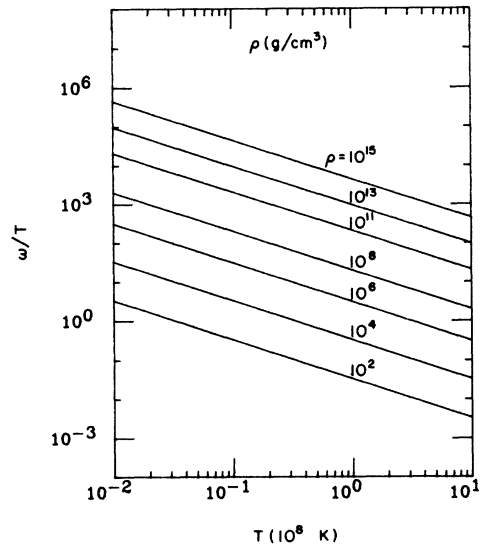

FIG. 2. The plasmon mass parameter ω/T as a function of temperature for various densities.

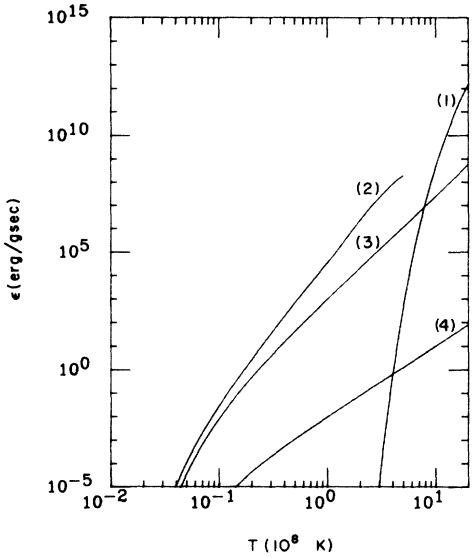

FIG. 4. Axion energy-loss rate as a function of temperature for $\rho=10^4$ g cm^{-3}, $\mu_e=\mu_e'=1$, and $m_a=1$ eV. (1) e^+e^-; (2) Compton; (3) Primakoff; (4) plasma decay.

where C is the chemical composition parameter, and ϵ_N is the total nuclear energy generation of the Sun.[12] The integrals ϵ_i are calculated numerically for the reactions (1)–(4) shown in Fig. 3. The function $M(r)$ can be found in Refs. 12 and 13.

We get $m_a<2.7$ eV or $v_\phi>1.3\times10^7$ GeV with a 10% estimated uncertainty due to ambiguity of solar models. Stars with larger masses burn at higher temperatures and have much larger nuclear energy generation rates resulting in a looser bound.

B. Helium-burning stars

Typical core temperatures of helium-burning stars are $T_c=1-2\times10^8$ K and densities $\rho_c=10^4-10^5$ g cm^{-3} for $M<5M_\odot$ (giants) or $\rho_c=10^3$ g cm^{-3} for $M\gtrsim15M_\odot$ (supergiants).[14] Plasmon effects are small since $\omega/T<1$, see Fig. 2, and the electron gas is at most mildly degenerate and approximately nonrelativistic. The energy generation rate from the 3α process is $\epsilon_N=10^2$ erg g^{-1}sec^{-1} and $\simeq5\times10^5$ erg g^{-1}sec^{-1} for giants and supergiants[14] and the condition $\epsilon_a<\epsilon_N$ gives $m_a<0.07$ and 1.05 eV, respectively. The energy loss comes mainly from the Compton process, see Fig. 4, while the annihilation and plasma decay processes give negligible contributions.

The above bounds depend on the adopted models of stellar evolution and cannot be trusted as model-independent results. However if the axion mass exceeds

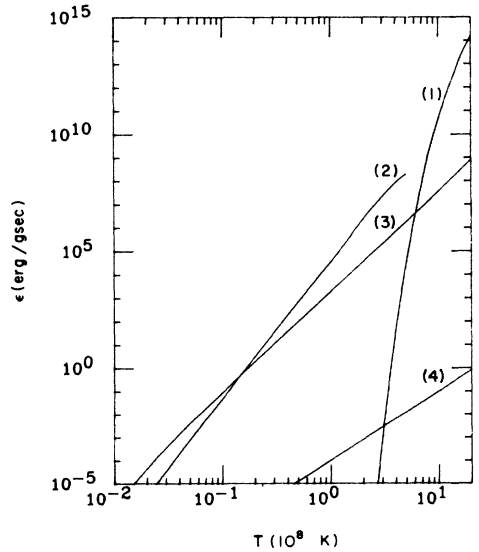

FIG. 3. Axion energy-loss rate as a function of temperature for $\rho=10^2$ g cm^{-3}, $\mu_e=\mu_e'=1$, and $m_a=1$ eV. (1) e^+e^-; (2) Compton; (3) Primakoff; (4) plasma decay.

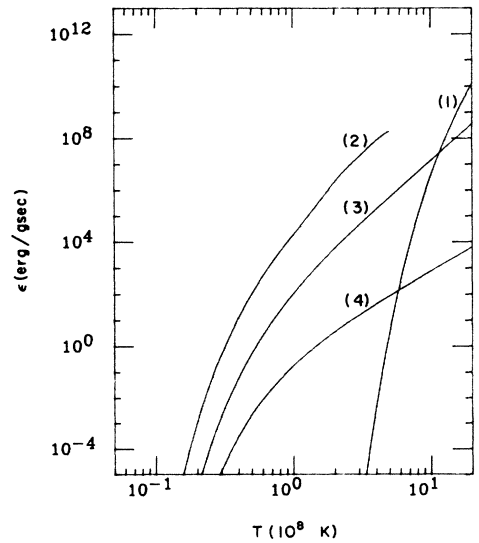

FIG. 5. Axion energy-loss rate as a function of temperature for $\rho=10^6$ g cm^{-3}, $\mu_e=\mu_e'=1$, and $m_a=1$ eV. (1) e^+e^-; (2) Compton; (3) Primakoff; (4) plasma decay.

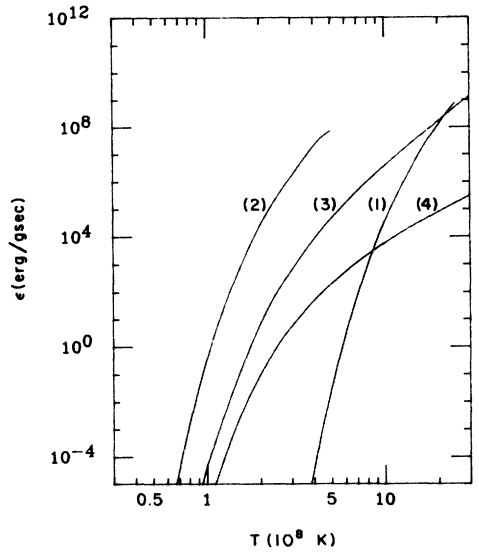

FIG. 6. Axion energy-loss rate as a function of temperature for $\rho=10^8$ g cm^{-3}, $\mu_e=\mu_e'=1$, and $m_a=1$ eV. (1) e^+e^-; (2) Compton; (3) Primakoff; (4) plasma decay.

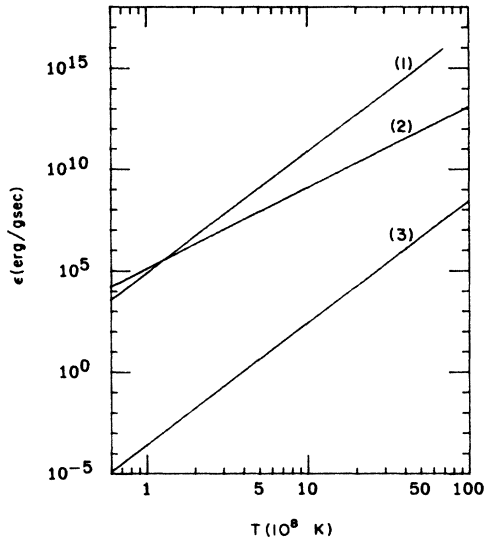

FIG. 8. Axion energy-loss rate as a function of temperature for $\rho=10^{13}$ g cm^{-3} and $m_a=1$ eV. (1) n-n bremsstrahlung; (2) Compton bremsstrahlung; (3) Primakoff bremsstrahlung.

these limits, the currently accepted scenario of stellar evolution will have to be drastically revised. At higher temperatures there is no such problem because the neutrino emission becomes more important if the axion mass is in the range of our interest.[15]

C. Carbon- and oxygen-burning stars

We examine here the white dwarfs of the Hyades for which Stothers[10] has found agreement between theoretical luminosity functions and the current data of luminosities unless the cooling due to neutrino emission is 10^2 times stronger. The stellar structure is simple with a uniform temperature $T_c\simeq 2\times 10^7$ K and $\rho_c=10^7$ g cm^{-3} for $M\simeq M_\odot$ and $\log_{10}L/L_\odot<-1.6$ (blue sequence). The low-mass sequence was not considered because the neutrino effects there are small. Here at core densities the plasma effects are very strong since $\omega/T\sim 30$ and electrons are very degenerate and relativistic. However, most of the contribution comes from the outer parts of the star, where $\rho\simeq 10^5$–10^6 g cm^{-3}, $\omega/T\sim 2$–10 and the electrons are degenerate and at most mildly relativistic, since the plasmon mass strongly suppress the momentum transfer to axions. Only the Compton process contributes significantly, see Figs. 5 and 6. The neutrino emission in this region is[16] 5×10^{-3} erg g^{-1}sec^{-1} and the condition $\epsilon_a<5\times 10^{-1}$ g^{-1}sec^{-1} gives $m_a<1.5$ eV. This bound is also model dependent with an estimated 20% uncertainty.

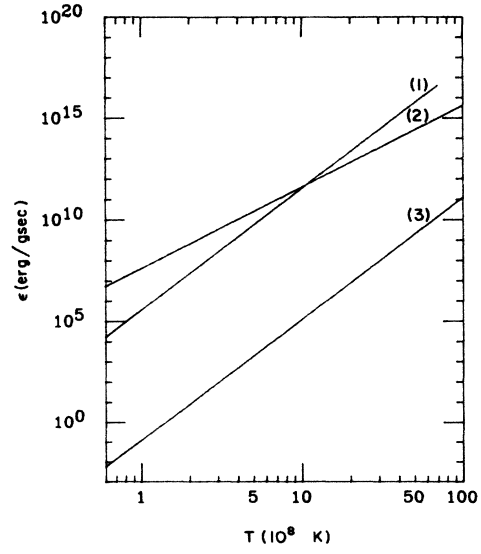

FIG. 7. Axion energy-loss rate as a function of temperature for $\rho=10^{11}$ g cm^{-3} and $m_a=1$ eV. (1) n-n bremsstrahlung; (2) Compton bremsstrahlung; (3) Primakoff bremsstrahlung.

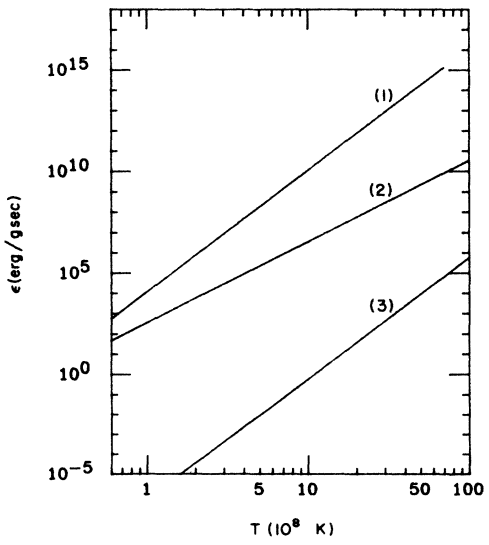

FIG. 9. Axion energy-loss rate as a function of temperature for $\rho=10^{15}$ g cm^{-3} and $m_a=1$ eV. (1) n-n bremsstrahlung; (2) Compton bremsstrahlung; (3) Primakoff bremsstrahlung.

TABLE I. Upper bounds on the axion mass.

Stellar object	Upper bound for m_a (eV)	Lower bound for v_0 (GeV)
Sun	$2.7\pm10\%$	10^7
Red giants	~0.07	$\sim5\times10^8$
Super giants	~1.05	$\sim4\times10^7$
Hyades	$1.5\pm20\%$	3×10^7
Supernovae	No bound	No bound
Neutron star crust	0.03–0.04	0.9–1.1×10^9
Neutron star core	2–3×10^{-3}	1.3–1.9×10^{10}

D. Supernovae

Supernovae have typical temperatures $T_c\sim10^9$–10^{12} K and densities $\rho_c\sim10^8$–10^{11} g cm^{-3}. The electron and positron gases are extremely relativistic and the e^+e^- annihilation processes are the dominant neutrino- and axion-production processes, the others being suppressed by electron degeneracy or plasmon effects. For an axion mass of the order of a few eV, the neutrino emission rate[15] is much higher than the axion rate, Eq. (2.12) so that

$$\frac{\epsilon_\nu}{\epsilon_a}>\frac{G_F^2M_e^4}{g^2\alpha}\left[\frac{\mu}{T}\right]^2\left[\frac{m_a}{\text{eV}}\right]^{-2}\gg1\ . \tag{3.2}$$

Thus no useful bound can be obtained in this case.

E. Neutron stars

We have a different physical picture in the case of neutron stars. With typical core densities $\rho_c\sim10^{15}$ g cm^{-3} and temperatures $T\sim10^8$–10^{10} K, plasmon effects ($\omega/T>100$, see Fig. 2) suppress all photoproduction processes, while the presence of positrons is negligible. The electron gas is extremely relativistic and completely degenerate while nucleons are approximately nonrelativistic and degenerate.

Following Iwamoto we choose two characteristic equations of state, by Bethe and Johnson[17] and by Pandharipande and Smith,[18] for neutron star matter. The neutrino emission from the dominant modified URCA process[8] $n+n\rightarrow n+p+e^-+\bar{\nu}_e$ and $n+p+e^-\rightarrow n+n+\nu_e$, is suppressed as the temperature goes down to 4.6×10^9 K due to proton superfluidity.[19] At lower temperatures the neutrino emission from the crust[20,21] becomes the dominant cooling mechanism. Comparing that rate with the neutron-neutron axion bremsstrahlung from the core, and taking the crust density to be $\rho\sim1.5\times10^{14}$ g cm^{-3} (we calculate the rates for $T=1$–4×10^9 K) we get $m_a<1.9$–2.8×10^{-3} eV, allowing two different equations of state. At even lower temperatures the neutrons also become superfluid[22] and at a temperature $T=2$–3×10^8 K photon radiation from the crust becomes the dominant mechanism. We compare at this temperature the Compton-type axion bremsstrahlung from the crust with the corresponding neutrino rate[20,21] (the Primakoff-type bremsstrahlung is always negligible) and demanding that $\epsilon_a<\epsilon_\nu$, we obtain $m_a<0.03$–0.04 eV. Again these results are model dependent but required in order to have consistency between experimental data[23] and the standard neutrino cooling scenario.[11] In Figs. 7–9 the axion emission rates due to the above three processes are compared for different densities. Nucleon superfluidity is not included.

IV. SUMMARY

We have calculated in detail axion emission rates in hydrogen-, helium-, carbon-, and oxygen-burning stars, neutron stars, and supernovae. The main reactions are photoproduction processes of Compton and Primakoff type, e^+e^- annihilation process, plasmon decay, and bremsstrahlung by electrons of Compton and Primakoff type and from neutron-neutron collisions. We get a qualitative agreement with the work of Fukugita, Watamura, and Yoshimura[3] but we obtain a stronger result for neutron stars. We summarize our results of the constraints on the axion mass for each and every case that we have considered in Table I. As discussed in the previous section, most of those results rely on our present understanding of stellar evolution and are model dependent. Even an axion mass of 3×10^{-3} eV may require a revision of the standard model of neutrino cooling for neutron stars. On the other hand, we find that axions would have no effect on gravitational collapse triggering supernovae explosions.

ACKNOWLEDGMENT

This work was supported in part by the U.S. Department of Energy under Contract No. DE-AC02-76ER03130.A016—Task A.

[1]R. D. Peccei and H. R. Quinn, Phys. Rev. Lett. **38**, 1440 (1977); F. Wilczek, *ibid.* **40**, 279 (1978); S. Weinberg, *ibid.* **40**, 223 (1978); G. 't Hooft, *ibid.* **37**, 8 (1976).

[2]M. Dine, W. Fischler, and M. Srednicki, Phys. Lett. **104B**, 199 (1981).

[3]M. Fukugita, S. Watamura, and M. Yoshimura, Phys. Rev. D **26**, 1840 (1982); Phys. Rev. Lett. **48**, 1522 (1982).

[4]N. Iwamoto, Phys. Rev. Lett. **53**, 1198 (1984).

[5]W. A. Bardeen and S. H. Tye, Phys. Lett. **74B**, 229 (1978).

[6]V. N. Tsytovich, Zh. Eksp. Teor. Fiz. **13**, 1775 (1961) [Sov. Phys. JETP **13**, 1249 (1961)]; J. B. Adams, M. A. Ruderman, and C.-H. Woo, Phys. Rev. **129**, 1383 (1963); see also K. Mikaelian, Phys. Rev. D **18**, 3605 (1978).

[7]G. Beaudet, V. Petrosian, and E. E. Salpeter, Astrophys. J. **150**, 979 (1967).

[8]B. L. Friman and O. V. Maxwell, Astrophys. J. **232**, 541 (1979).

[9]Iwamoto of Ref. 4, calculated the spin-summed matrix element, however, based on the nonrelativistic one-pion-exchange potential. In our relativistic treatment the

pseudoscalar-axion-nucleon coupling interferes with the pion-nucleon coupling and the matrix element depends on $M_N^2 |\mathbf{P}_1 - \mathbf{P}_3|^2$, etc., differently compared to Iwamoto's result; G. Da Prato, Nuovo Cimento **22**, 123 (1961).

[10]R. B. Stothers, Phys. Rev. Lett. **24**, 538 (1970).

[11]K. Nomoto and S. Tsuruta, Astrophys. J. Lett. **250**, L19 (1981).

[12]D. Clayton, *Principles of Stellar Evolution and Nucleosynthesis* (McGraw-Hill, New York, 1968).

[13]J. N. Bahcall and G. Shaviv, Astrophys. J. **153**, 11 (1968); **153**, 3 (1968).

[14]See, for example, K. Sato and H. Sato, Prog. Theor. Phys. **54**, 1564 (1975); D. A. Dicus, E. W. Kolb, V. L. Teplitz, and R. V. Wagoner, Phys. Rev. D **18**, 1829 (1978).

[15]D. A. Dicus, Phys. Rev. D **6**, 941 (1972); also Ref. 7.

[16]S. C. Vila, Astrophys. J. **146**, 437 (1966); **149**, 613 (1967); M. P. Savedoff, H. M. Van Horn, and S. C. Vila, *ibid.* **155**, 221 (1969).

[17]H. A. Bethe and M. B. Johnson, Nucl. Phys. **A230**, 1 (1974).

[18]V. R. Pandharipande and R. A. Smith, Nucl. Phys. **A237**, 507 (1975); V. R. Pandharipande *et al.*, Astrophys. J. **208**, 550 (1976).

[19]N. C. Chao, J. W. Clark, and C. H. Yang, Nucl. Phys. **A179**, 320 (1972).

[20]G. G. Festa and M. A. Ruderman, Phys. Rev. **180**, 1227 (1969); D. A. Dicus, E. W. Kolb, D. N. Schramm, and D. L. Tubbs, Astrophys. J. **210**, 481 (1976).

[21]M. Soyeur and G. E. Brown, Nucl. Phys. **A324**, 464 (1979).

[22]T. Takatsuka, Prog. Theor. Phys. **48**, 1517 (1972).

[23]D. J. Helfand and R. H. Becker, Nature (London) **307**, 215 (1984).